TECHNICAL TRANSACTIONS | **CZASOPISMO TECHNICZNE**
ELECTRICAL ENGINEERING | ELEKTROTECHNIKA
2-E/2015

WOJCIECH WROŃSKI*, MACIEJ SUŁOWICZ*, ARKADIUSZ DZIECHCIARZ**

DYNAMIC AND STATIC ECCENTRICITY DETECTION IN INDUCTION MOTORS IN TRANSIENT STATES

DIAGNOSTYKA EKSCENTRYCZNOŚCI DYNAMICZNEJ I STATYCZNEJ W SILNIKU INDUKCYJNYM W PRZEJŚCIOWYM STANIE PRACY

Abstract

The following paper presents possibilities for the application of selected time-frequency analysis methods in the fault detection of cage induction machines in transient states. The starting phase current of the machine was chosen as a diagnostic signal. Selected faults were eccentricities – static and dynamic. In order to increase the selectivity of the obtained signal transformations, a notch filter was used to remove the base harmonic of the phase current. Two approaches of fault detection were compared. In the first approach, the characteristic feature of fault was extracted using DWT analysis. Next, TMCSA methodology was applied in which characteristic harmonics related to faults were shown on a time-frequency plane. In this case, applied methods were a Gabor transformation, STFT, CWT and Wigner–Ville's transformation. In the analysis, a phase current signal approximated by DWT was used. DWT approximation was applied to filter higher harmonics which improves the resolution of the obtained transformations.

Keywords: *cage induction motor fault detection*, *TMCSA*, *time-frequency methods*, *Notch filter*, *transient phase current*, *dynamic and static eccentricity*, *voltage asymmetry*

Streszczenie

W artykule przedstawiono możliwości zastosowania wybranych metod analizy czasowo-częstotliwościowej do diagnostyki uszkodzeń silników indukcyjnych klatkowych w przejściowych stanach pracy. Jako sygnał diagnostyczny wybrano prąd fazowy silnika podczas rozruchu. Wybranymi przypadkami uszkodzeń silnika są ekscentryczność statyczna i dynamiczna. W celu poprawienia selektywności otrzymanych transformat wykorzystano filtr Notcha do usunięcia harmonicznej podstawowej prądu. Porównano dwa podejścia diagnostyczne wykrywania uszkodzeń. Pierwsze za pomocą analiz wielorozdzielczych z użyciem DWT, polegające na wyróżnieniu charakterystycznego wzorca związanego z uszkodzeniem. Drugie podejście polegało na zastosowaniu metodologii TMCSA, czyli ekstrakcji charakterystycznych harmonicznych związanych z uszkodzeniami zależnych od poślizgu na płaszczyznach TF. W tym wypadku rozważanymi metodami analizy były transformacje Gabora, STFT, Wignera–Ville'a oraz CWT. Do tych analiz został wykorzystany sygnał prądu aproksymowany z użyciem DWT, w celu odfiltrowania widma czasowo-częstotliwościowego o wyższych częstotliwościach, aby poprawić rozdzielczość otrzymywanych transformat.

Słowa kluczowe: *silnik indukcyjny klatkowy*, *diagnostyka uszkodzeń*, *TMCSA*, *metody czasowo-częstotliwościowe*, *filtr notch*, *prąd fazowy w stanie przejściowym*, *ekscentryczność statyczna i dynamiczna*, *niesymetria napięć*

DOI: 10.4467/2353737XCT.15.095.3927

* M.Sc. Eng. Wojciech Wroński, Ph.D. Eng. Maciej Sułowicz, Department of Electrical and Computer Engineering, Institute of Electromechanical Conversion, Cracow University of Technology.

** M.Sc. Eng. Arkadiusz Dziechciarz, Technical University of Cluj-Napoca, Faculty of Electrical Engineering.

1. Introduction

This paper presents possibilities for the application of selected time-frequency methods of signal analysis in fault detection of cage induction machines in transient states. Fault diagnosis of induction motors using Fourier transformation or FFT algorithms, can be used only in steady states because it is a frequency analysis method of signals. Because of that, this method is insufficient in the case of transient states when diagnostic signals related to faults vary in time. Applying time-frequency methods of signal analysis allows for analyzing time changing diagnostic signals related to faults of induction motors in transient states.

In this paper, methodology of static and dynamic eccentricity detection in transient states and with supply voltage asymmetry will be presented. Supply voltage asymmetry will be considered as distortion in eccentricity detection which has not yet been presented in literature. Two approaches of fault detection will be compared – using multi-resolution analysis with DWT and analysis on TF planes using Gabor transform, STFT, CWT and Wigner–Ville's transform which use TMCSA (transient motor current signature analysis) methodology that is the extraction of characteristic slip dependent harmonics related to faults. The selected diagnostic signal is a stator phase start-up current. In order to improve selectivity of the obtained transforms, a notch filter was used to remove the base harmonic of the current of frequency equal to that of the supply voltage.

2. Measurement system and data capturing

For cage induction machine diagnosis using selected methodology, it is necessary to collect diagnostic signals of phase current and rotational speed. A waveform of rotational speed will be used to find the actual harmonics related to faults in the case of analysis on a TF plane – this makes it easier to localize these harmonics. The examined cage induction motor Sg112-M4 was supplied directly from the network and is connected with a DC generator. The schematics of the system for fault detection is shown in Fig. 1.

Parameters of examined motor are: $P_N = 4$ kW; $U_N = 380$ V; $I_N = 2.867$ A; $\cos\varphi_N = 0.84$; $n_N = 1445$ rpm; Number of rotor bars – $N_r = 28$.

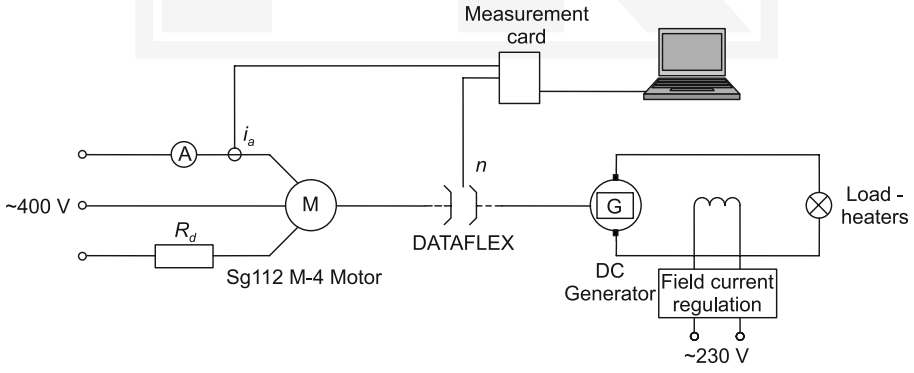

Fig. 1. System of cage induction motor fault detection

The dynamic eccentricity of the motor is realized by using a special replaceable rotor with steel sheets non-centrically placed on the shaft. Static eccentricity is realized by specially prepared bearing shields with a shifted center of symmetry axis.

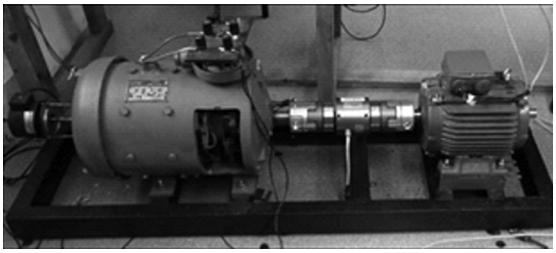

Fig. 2. Laboratory test bench

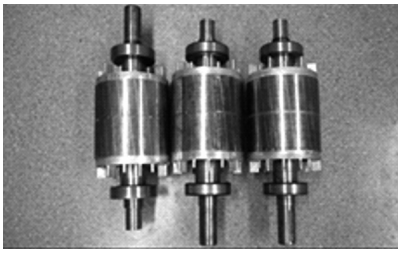

Fig. 3. Set of exchangeable rotos

Voltage asymmetry was realized by the connecting of additional resistor R_d to one phase of the stator. For the collecting of the current signal, current transducer LEM HY 15 was used, and for rotational speed signal collecting, DATAFLEX® 22/5 transducer was used.

The following diagnostic data were collected for nominal load ($I \cong 3$ A) of the machine:

- healthy motor (i_sym),
- dynamic eccentricity (i_de),
- static eccentricity (i_se),
- static eccentricity and supply voltage asymmetry (i_senn).

3. Selected methods of signal analysis

In the case of non-stationary signals, their characteristic features vary in time. In this case, Fourier transform proves to be insufficient because the spectra of those signals vary in time and the Fourier analysis gives averaged results (in the analysis window). The solution for this inconvenience was proposed by Gabor as a short time Fourier transform STFT and next introduction and development of wavelet transform methods [4].

Frequency analysis of non-stationary signals should be performed using a base of decomposition contained of selective functions in time and frequency domain. The signal's decomposition is made by shifting the analyzing function in the time domain and modulation in the frequency domain. Impulse waveforms are used for this because in the time domain, it decides the time range of the analysis and in the frequency domain, its spectrum decides the frequency range of the analysis [2].

Because each of the impulse waveforms covers a specified time and frequency range, some amount of signal for a certain time-frequency cell is selected. Areas of those cells should not intersect with each other, and when summed up, should be equal to the time-frequency plane area. Two basic strategies for time-frequency plane division and corresponding chessboards are presented in Figure 4 [1].

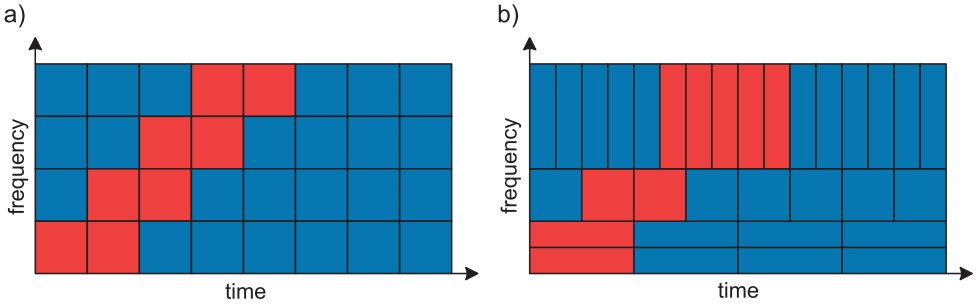

Fig. 4. Base chessboards of time-frequency decomposition of signals: Gabor's transform–Short Time Fourier Transform (a);wavelet transform (b). Red shows non-zero coefficients of the example time-frequency decomposition of the signal with the frequency changing linearly [1]

3.1. Gabor's transform

According to [1], in the time-frequency Gabor transform, the analyzed signal is introduced as a sum of the base functions which are derived from the prototype function i.e. the Gaussian window, by shifting it in the time and frequency domain. The TF atom of the prototype function is localized in the time-frequency space around point ($t = 0, f = 0$) and is of a random shape. As a result of the prototype function shifting, we obtain the TF decomposition structure analogous to that presented in Fig. 4a). In Gabor's decomposition, the area and orientation of the TF atoms are constant.

The time-frequency Gabor decomposition of the continuous signalis defined as [1]:

$$x(t) = \sum_{m,n=-\infty}^{+\infty} c_{m,n} g_{m,n}(t) \tag{1}$$

where $g_{m,n}(t)$ means time shifted by $m \cdot \Delta t$ and frequency shifted by $n \cdot \Delta f$ any base function (prototype) $g(t)$ of energy equal to one (Δt, Δf – specified translation in time and frequency domain) [1]:

$$g_{m,n}(t) = g(t - m \cdot \Delta t) e^{j2\pi(n \cdot \Delta f)t}, \quad \Delta t \cdot \Delta f \leq 1 \tag{2}$$

and $c_{m,n}$ are decomposition coefficients, calculated from equation [1]:

$$c_{m,n} = \int_{-\infty}^{+\infty} x(t) \gamma_{m,n}^{*}(t)\, dt, \; \gamma_{m,n}(t) = \gamma(t - m \cdot \Delta t) e^{j2\pi(n \cdot \Delta f)t} \tag{3}$$

In equation (3), $\gamma(t)$ is a prototype function (window) of analysis which has to be biorthogonal to the synthesis prototype function (window g(t) (2). Because the base function $g(t)$ should have a large energy concentration both in the time and frequency domain, the most commonly used function is a Gaussian window. Equation (3) is an analysis equation (signal $x(t) \rightarrow$ decomposition coefficients $c_{m,n}$), and (1) − synthesis equation (decomposition coefficient $_{cm,n} \rightarrow$ signal $x(t)$). Because we use the same window g(t) area and shape of the TF atom related to functions $g_{m,n}(t)$ are constant. As a result of the window translation in the time and frequency domain, we obtain the chessboard of decomposition presented in Fig. 4a) [1].

The time-frequency Gabor's representation of continuous signal $x(t)$ is defined as [1]:

$$S_x(mT, nF) = \left| c_{m,n} \right|^2 \tag{4}$$

3.2. STFT transform

In [13], the application of STFT(short time Fourier transformation) was described as a solution to the problem of localization of the feature occurring in the diagnostic signal in time. This transform, apart from frequency analysis, allows localizing the characteristic frequency components occurring in time, using time windows.

According to [1],the continuous, short time Fourier transform STFT can be considered as non-discretized in time and frequency domain Gabor transform. High redundancy is typical for this transform. During analysis and synthesis, the same window is used.

The definition of this transform in time and frequency domain [1]:

$$\mathrm{STFT}_x^T(t, f) = \int_{-\infty}^{+\infty} x(\tau)\gamma^*(\tau - t)e^{-j2\pi f\tau}d\tau \tag{5}$$

The spectrogram related to the STFT is defined as[1]:

$$S_x^{\mathrm{SPEC}}(t, f) = \left| \mathrm{STFT}_x(t, f) \right|^2 \tag{6}$$

In [2] it is given, that the spectrogram is usually obtained using one of the basic windows: rectangular; Hamming; Hanning; and others.

In the STFT wide window, $\gamma(t)$ increases the resolution in the frequency domain and decreases the resolution in the time domain. The narrow window does exactly the opposite. It is impossible to obtain a high resolution in both domains simultaneously [1].

3.3. Wigner–Ville's transform

In the transforms of Gabor and STFT presented so far, the problem of a proper size window selection forced to compromise between the precision of the analysis and the analysis of the entire spectrum of components contained in the signal. This problem is a basic drawback of time-frequency analysis until the window of a varying length was used. An attempt of adapting the selection of the window size for the local features of the signals, is made in Wigner–Ville's transform. In this transform, the signal also plays the role of the window [2].

The time-frequency transform of the Wigner–Ville (WV) perfectly shows the linear change of frequency in the TF space. The transform of the Wigner–Ville is defined as [1]:

$$\mathrm{WV}_x(t, f) = \int_{-\infty}^{+\infty} x\left(t + \frac{\tau}{2}\right) x^*\left(t - \frac{\tau}{2}\right) e^{-j2\pi f\tau}d\tau \tag{7}$$

where $x(t)$ is a real signal (Wigner's definition) or analytical (Ville's definition). The analytical signal (8), related to the real signal $x(t)$, is a complex signal whose real part is signal $x(t)$ and the imaginary part is a result of the Hilbert transform of $x(t)$ of [1, 5]:

$$z(t) = x(t) + jH[x(t)] \tag{8}$$

The transform of Wigner–Ville solves the problem of the window size selection for analysis. All components contained in the signal are analyzed, each of them is localized with optimal time precision as precisely as is possible due to Heisenberg's uncertainty theorem [2]. In [4] it is proved that the resolution of the WV transform is twice as large as that of the STFT.

The basic drawback of the WV transform is the interference in the obtained time--frequency spectral matrices.

3.4. Wavelet transform

The wavelet transform is one of the most popular and most dynamically developed methods of time-frequency analysis of non-stationary signals and is a method with constant percentage bandwidth $\Delta f/f_0 = \text{const}$ [1].

The development of this transform is a result of the increased demand for time-frequency analysis of variable window size which could provide high frequency resolution for low-frequency components and accurate time localization for high-frequency components of transient signals [4].

3.4.1. Continuous wavelet transform CWT

Continuous wavelet transform of signal $x(t)$ is defined in the time and frequency domain in the following way [1]:

$$\mathrm{CWT}_x^T(t,a) = \frac{1}{\sqrt{|a|}} \int_{-\infty}^{+\infty} x(\tau)\gamma^*\left(\frac{\tau - t}{a}\right) d\tau \tag{9}$$

The division by $|a|$ keeps the wavelets' energy constant after rescaling. The function $\gamma(t)$ is an analyzing function [1].

Scalogram, related to the wavelet transform is defined in the following way [1]:

$$S_x^{\mathrm{SCAL}}(t,a) = \left|\mathrm{CWT}_x(t,a)\right|^2 \tag{10}$$

In [3], the problem of interpretation scale-frequency relation, concerning the sampling frequency, was introduced. The dependence describing the central frequency of the base wavelet $\gamma(t)$ is of the following form [3]:

$$\omega_0 = \frac{1}{2\pi} \int_0^{\infty} \omega \left|\Phi(\omega)\right|^2 d\omega \tag{11}$$

where:

$\Phi(\omega)$ – Fourier transform of $\varphi(t)$.

Furthermore, the bandwidth of the base wavelet, which can be related to the Heisenberg cube in the direction of frequency axis, is of the form [3]:

$$B_0 = \omega_{\max} - \omega_{\min} \tag{12}$$

For small scale coefficients, the wavelet transform extracts the high frequency components of the analyzed signal and for larger scale coefficients, the effect is exactly the opposite. While the scale coefficient increases, the frequency bandwidth decreases, this

means that the resolution in the frequency domain is greater. The central frequency ω_0 and bandwidth B_0 depend on the chosen analyzing wavelet [3].

3.4.2. Discrete wavelet transform DWT

The continuous wavelet transform gives a lot of redundant information. This is why its parameters such as time t and scale coefficient a are sampled obtaining the coefficient of the wavelet series analogically to the Fourier series [2, 4].The DWT has a constant TF atom and realizes the time-frequency signal decomposition scheme presented in Fig. 4b) [2].

The discrete wavelet transform is strictly related to the multi-resolution signal analysis [2]. Example of three level discrete wavelet analysis with wavelet filters is presented in Fig. 5,where h_d is a low-pass filter, corresponding to scaling function, h_g is a high-pass filter corresponding to the wavelet function [4]. Since the calculation of wavelet coefficients $c_{m,n}$ and $d_{m,n}$ from their definition is very difficult, in practice, we use filters related to the wavelet and scaling functions [2, 4].

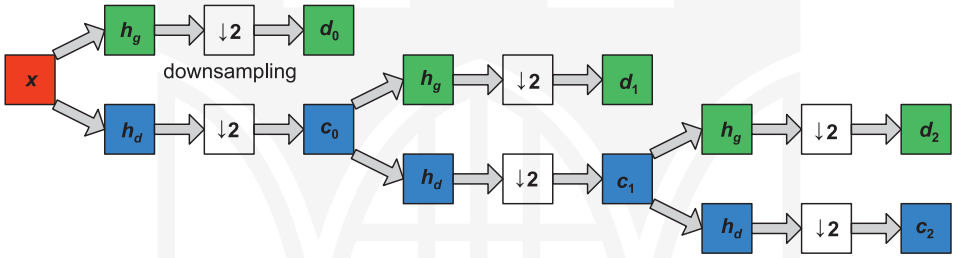

Fig. 5. Three level discrete wavelet analysis using wavelet filters [4]

DWT allows writing signal $x(t)$ as a sum of approximation a_n and details d_j [10]:

$$x(t) = a_n + d_n + \cdots + d_1 \tag{13}$$

where [10]:

- n – level of decomposition,
- a_n – approximation of signal on level n,
- d_j – detail of signal on level j.

Equation(13) realizes Mallat's algorithm which shows that each wavelet signal is related to a specified frequency bandwidth. If F_s (in samples per second) is sampling the frequency of the analyzed signal $x(t)$, then the detail of signal d_j contains information concerning the signal's components of frequencies from interval [8, 10]:

$$f(d_j) \in [2^{-(j+1)} F_s,\ 2^{-j} F_s]\ \text{Hz} \tag{14a}$$

approximation a_n contains low frequency components that belong to interval [8, 10]:

$$f(a_n) \in [0,\ 2^{-(n+1)} F_s]\ \text{Hz} \tag{14b}$$

The DWT performs filtration process shown in Fig. 6.

Filtration is not ideal, which causes the adjacent bandwidths to interfere. This may become an issue since some frequency components (base harmonic) might be partially

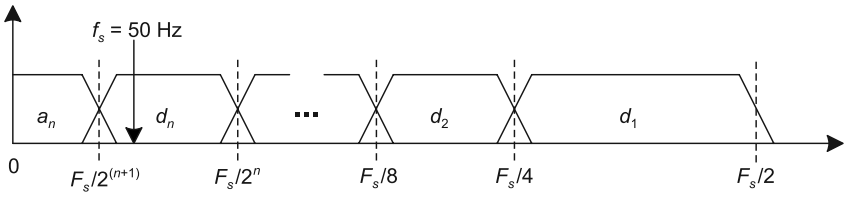

Fig. 6. Filtration process performed by DWT [8, 10]

filtered in an adjacent bandwidth covering other frequency components in this bandwidth [10].

4. Methodology of induction machines' diagnosis using time-frequency analysis methods

4.1. Application of induction motors' diagnosis methods in transient state based on TMCSA

The presented methodology of induction motors fault detection is based on the TMCSA method.

In recent years, methods of electrical machine diagnostics in transient states became of more interest. A variety of methods based on transient stator current analysis were proposed. Those methods are known as TMCSA (transient motor current signature analysis), and can be described as a generalization of traditional MCSA methods applied for diagnostics in steady states. The well-known MCSA methods are based on stator current's Fourier spectrum analysis in steady states. Theoretical experiments prove that different types of faults in electrical machines generate or amplify some frequency components in stator currents related to particular faults of the machine [7].

TMCSA uses methods of non-stationary signals analysis. Signal forming can be performed with wavelet analysis or through using filters. Spectral analysis is performed on the time-frequency plane using linear transforms like STFT and wavelet transform or square transform such as Wigner–Ville's transform [11].

In concluding, TMCSA is a technology which allows diagnosing the motor by analyzing the current during rotational speed change. Diagnostics with TMCSA are, in general, based upon the extraction of typical components on the TF plane related to particular types of faults. These methods replace traditional methods based of the Fourier transform which are not dedicated for the analysis of signals in transient states [6].

The presented method of diagnosis was based on performing the following analyses:

– First, the diagnostic signal of stator phase currentwas processed by notch filtering order to filter the base harmonic of the frequency equal to that of supply voltage.

Next, for such a prepared signal, two approaches of fault detection were compared:

– Multi-resolution signal analysis was performed with DWT in order to extract typical components related to faults.

– Time-frequency analyses on the TF plane was performed using various transforms – Gabor's, STFT, Wigner–Ville' sand CWT, in order to extract characteristic harmonics related to faults. Approximation signal obtained from DWT will be used for analysis.

4.2. Application of notch filter

In the presented approach, a notch filter was used for the initial filtration of the measured current signal, to increase the selectivity of the transforms and better distinguishing of harmonics related to faults, by removing the base harmonic of the frequency equal to that of supply voltage.

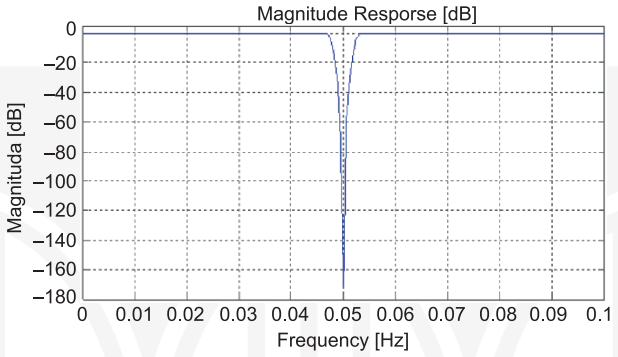

Fig. 7. Frequency characteristic of designed Notch filter

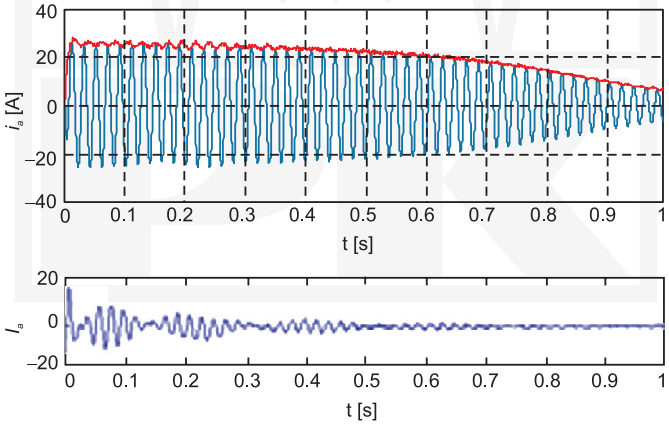

Fig. 8. Current waveform i_sym (top) and after filtration with the notch filter (bottom)

The notch filter, which is of IIR type, designed for certain frequency, removes that harmonic of signal. Input parameters of this filter are cut-off frequency$F0$, and frequency bandwidth 3-dB BW or quality factor Q. For these specifications, by increasing filter order N, one can obtain a filter closer to the ideal [14].

For the applied notch filter, in order to remove the base harmonic, the following parameters were chosen:

– $N = 10$ – filter order.
– $F0 = 50$ Hz – cutoff frequency,
– $BW = 5$ Hz – bandwidth 3-dB,
– $Q = F0/BW$ – obtained quality factor.

In the picture below, there is presented frequency characteristic of the designed notch filter. Obtained attenuation of base harmonic reaches 170 dB.

In the picture below, there is presented an example waveform of the motor's current for healthy motor, and with filtered base harmonic using the designed notch filter. It is not an ideal filtration and base harmonic is partially present in analyzed signal.

4.3. DWT based diagnostic approach

A diagnostic approach based on the DWT will be used in the case of a multi-resolution analysis perform. In [8] a general scheme of a DWT based method for eccentricity detection based on transient current analysis was presented. It allows for extraction in the transient state characteristic harmonics that are related to fault occurrence. These typical harmonics are reliable for fault detection because it is very less likely that a specific waveform of a particular harmonic in transient state was caused by a different phenomenon unrelated to the fault. Moreover, those harmonics allow distinguishing particular faults based on waveforms contained in wavelet signals.

In this paper, this approach is used to detect previously mentioned faults. In Figure 9, a scheme of DWT based methodology for fault detection in the induction machine is presented [8].

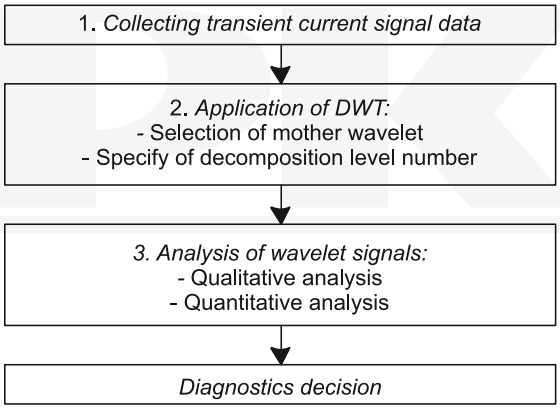

Fig. 9. Methodology scheme of DWT based diagnostic [8]

1. Collecting current signal's samples in transient state

Collected current signal in transient state is a basic signal for diagnosis. The standard sampling frequency of data acquisition device equal to 2 or 5 kS/s ensures a good

resolution according to equations (14a and b), introducing different sets of frequency bandwidths [8].

In the performed analyses, the sampling frequency was equal to F_s = 5 kS/s.

2. Application of DWT

Before using DWT, mother wavelet and the number of decomposition levels must be specified [8].

1) Choice of mother wavelet

Daubechies wavelet of 45order ('db45') was chosen for the analysis. According to [8], this kind of wavelet of an order higher than 20 gives satisfying results.

2) Specifying number of decomposition levels

The number of decomposition levels depends on the desired low frequency components. Waveforms of these components are represented by DWT signals of high level [8].

In the case of examined faults, low frequency components are not taken into account.

In order to find number of decomposition levels n_f equation, that describes approximation a_{nf} level below supply frequency [8, 9]:

$$n_f = \text{integer}\left[\frac{\log(F_s / f_s)}{\log(2)}\right] \tag{15}$$

For F_s = 5000 samples per second and f_s = 50 Hz, we obtain a level of decomposition equal to n_f = 6. Using equations (14a and b) bandwidths for specified sampling frequency for each DWT signal are presented in Table 1. [8].

Table 1

Frequency bandwidths of DWT signals for F_s = 5000 S/s [8]

Level	Bandwidth [Hz]
d1	1250–2500
d2	625–1250
d3	312.5–625
d4	156.25–312.5
d5	78.12–156.25
d6	39.06–78.12
a6	0–39.06

Using this distribution of wavelet signals allows following changes related to different faults.

3. Analysis of wavelet signals

The next step is to perform qualitative and quantitative analysis in order to evaluate the obtained DWT decomposition signals [8].

1) Qualitative analysis

The purpose of qualitative analysis is to detect the presence of characteristic components caused by slip dependent fault harmonics. It is obtained by analyzing oscillations that occur in wavelet signals [8].

2) Quantitative analysis

When the machine's condition is initially diagnosed, using qualitative identification of characteristic components, it is possible calculate quantitative parameters of particular faults in order to evaluate the degree of damage to the machine [8].

For the performed analyses, the following quantitative factors were assumed:

– In the case of the multi-resolution DWT analysis, the percentage energy E of wavelet signals and percentage energy differences [13]:

$$W = \left| \frac{E_z - E_u}{E_z} 100\% \right| \tag{16}$$

where:

E_z, E_u – energy of signal with and without fault.

In this case, detail d6 containing base harmonic is omitted.

– For time-frequency analyses – energy of the harmonic related to the fault obtained from transform E [dB] and absolute energy difference:

$$\Delta E = \left| E_z - E_u \right| \text{ [dB]} \tag{17}$$

4. Diagnostic decision

When qualitative patterns related to faults are defined and the quantitative degree of damage is specified, it is possible to make a diagnostic decision [8].

4.4. Detection of dynamic and static eccentricity

The problem of dynamic and static eccentricity detection using TMSCA method has not yet been fully examined. This paper presents attempts for the detection of these faults in transient states of the machine during start-up.

In [12], for monitoring of the stator winding condition and also the supply voltage asymmetry considered as distortion in static eccentricity detection, amplitude of frequency component was presented.

$$f_{nn} = 3 f_s \tag{18}$$

Also, harmonics that prove the presence of dynamic and static eccentricity, respectively in low and medium frequency bandwidths were presented [12]:

$$f_{ednn}(s) = f_s \left(k \frac{1-s}{p} \pm m \right) \tag{19}$$

$$f_{esnn}(s) = f_s \left(k N_r \frac{1-s}{p} \pm m \right) \tag{20}$$

where:

$k = 1, 2, 3, \ldots,$

$m = 1, 3, 5, \ldots,$

In Figure 10, spectrum of stator current in phase A, for nominal load ($I \cong 3$ A) supplied form voltage of frequency $f_s = 50$ Hz, in steady state – MCSA method, for healthy motor Fig. 10a, dynamic eccentricity occurrence Fig. 10b, static eccentricity occurrence Fig. 10c and static eccentricity occurrence with voltage asymmetry Fig. 10d. Once can observe the increase of odd multiples of network frequency and increase of harmonics described by (19) for $k = 1$ and $m = 3$ and by (20) for $k = 1$ and $m = 1$[12].

These harmonics that are typical for eccentricity occurrence are also present in a healthy motor and are equal to frequency components caused by load variations. For that reason, eccentricity detection is more difficult [12].

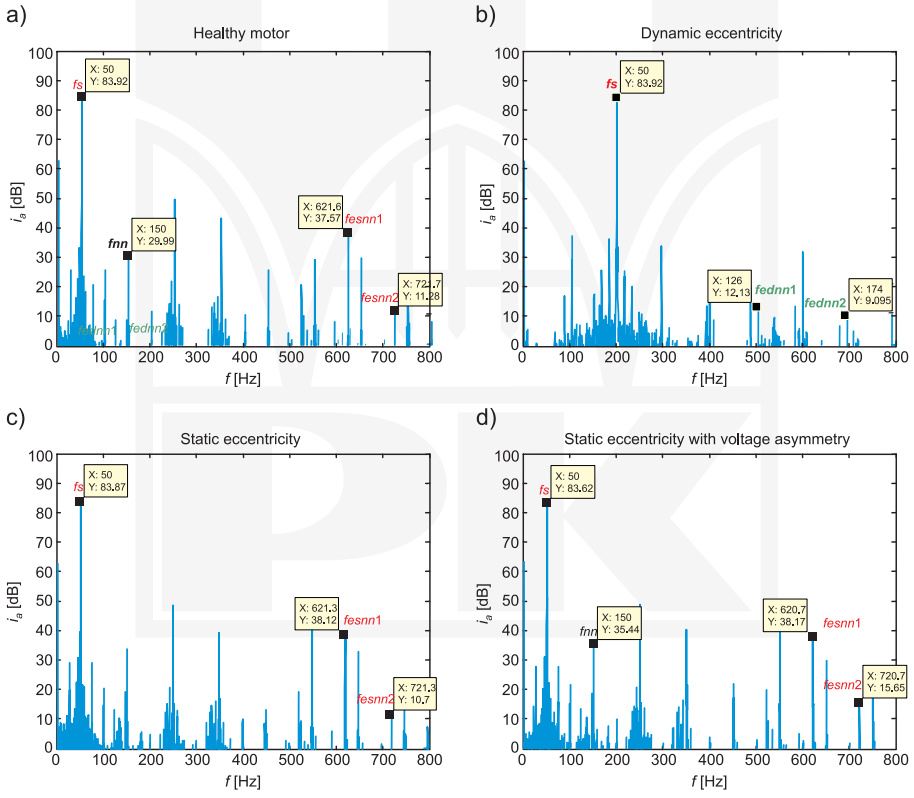

Fig. 10. Stator current spectrum of loaded machine (nominal load) with $Fs = 50$ Hz and a) no fault, b) dynamic eccentricity, c) static eccentricity, d) static eccentricity with voltage asymmetry [12]

The attempt of eccentricity detection is made using the TMCSA method, using the following harmonics (indexes mean different variants of the equation: 1 for „–”, 2 for „+”):

– dynamic eccentricity: (19) for $k = 1$ and $m = 3$: $f_{ednn1,2}$,
– static eccentricity: (20) for $k = 1$ and $m = 1$: $f_{esnn1,2}$,
– supply voltage asymmetry: (18) f_{nn}; (19) for $k = 1$ and $m = 3$: $f_{ednn1,2}$; (20) for $k = 1$ and $m = 1$: $f_{esnn1,2}$.

Characteristic patterns of harmonics are shown in the picture below on the slip--frequency plane (where the slip is replaced by a rotational speed for a motor with four poles $p = 2$):

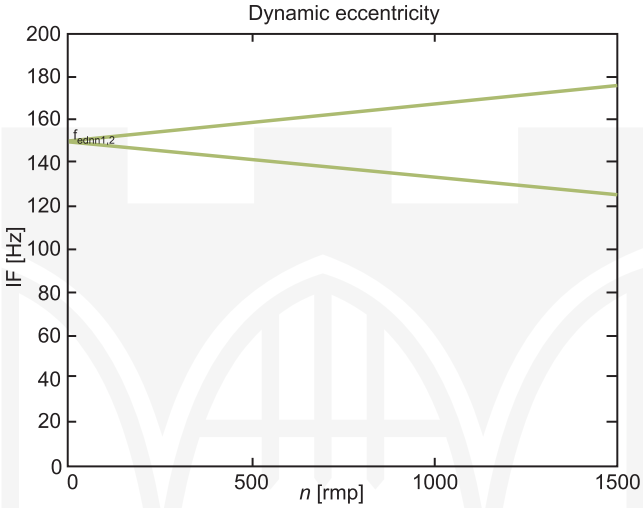

Fig. 11. Characteristic harmonics for dynamic eccentricity on slip-frequency plane

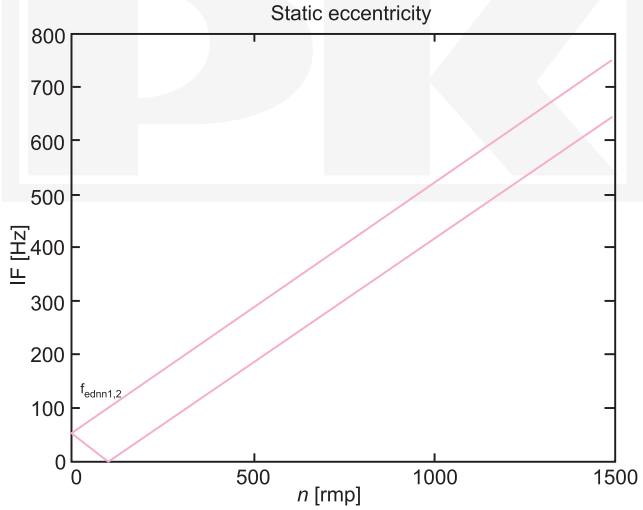

Fig. 12. Characteristic harmonics for static eccentricity on slip-frequency plane

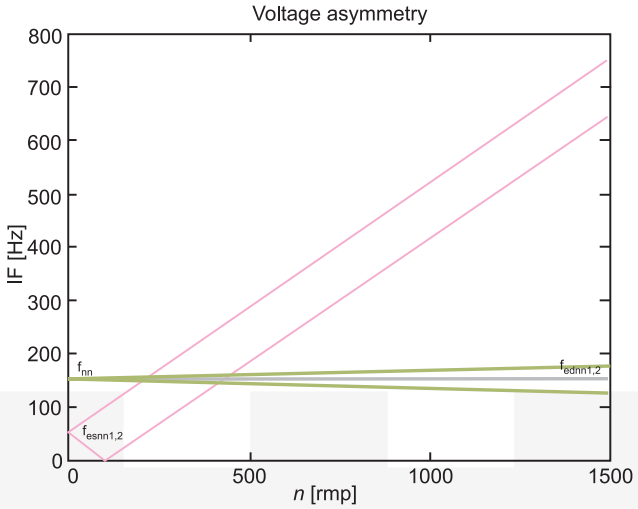

Fig. 13. Characteristic harmonics for voltage asymmetry on slip-frequency plane

In the case of using DWT for multi-resolution analysis, for sampling frequency set to F_s = 5000 samples per second and decomposition level of the current signal equal to n_f = 6, according to equation (15) in obtained frequency bandwidths of DWT wavelet signals, presented in Table 1, characteristic components related to fault occurrence will be sought. Bandwidths of DWT with contained harmonics are presented in Table 2.

Table 2

Frequency bandwidths of DWT signals for F_s = 5000 S/s for diagnosis of dynamic eccentricity (ED), static eccentricity (ES) and voltage asymmetry (NN)

Level	Bandwidth [Hz]	Characteristic harmonics		
		ED	ES	NN
d1	1250–2500			
d2 (a1)	625–1250		$f_{esnn1,2}$	$f_{esnn1,2}$
d3 (a2)	312.5–625		$f_{esnn1,2}$	$f_{esnn1,2}$
d4 (a3)	156.25–312.5	f_{ednn2}	$f_{esnn1,2}$	$f_{ednn2}, f_{esnn1,2}$
d5 (a4)	78.12–156.25	$f_{ednn1,2}$	$f_{esnn1,2}$	$f_{nn}, f_{ednn1,2}, f_{esnn1,2}$
d6 (a5)	39.06–78.12		$f_{esnn1,2}$	$f_{esnn1,2}$
a6	0–39.06		f_{esnn1}	f_{esnn1}

* approximations relating to upper frequency limits of particular details are given in parenthesis

One can notice that bandwidth containing harmonics related to faults in the case of dynamic eccentricity includes DWT signals d4 and d5, and for static eccentricity with voltage asymmetry, from d2 to a6. Analysis of detail d6 is omitted since it contains base harmonic.

For particular fault cases, DWT approximations of the current signal for the analyses on the TF planes, are obtained from the following signals of wavelet transform performed using Daubechies wavelet of 45th order ('db45'):

- dynamic eccentricity: a3,
- Static eccentricity: a1,
- Voltage asymmetry: a1.

5. Results of analyses of particular fault cases

The following analyses were performed:

- *Multi-resolution analysis with DWT*
  - Dynamic eccentricity detection (ED): analysis of wavelet signals d4 and d5 (for wavelet filter: 'db45').
  - Static eccentricity detection (ES) and voltage asymmetry (NN): analysis of wavelet signals d2 – a6 (for wavelet filter: 'db45').
- *Time frequency analyses on TF planes*

  Energy of characteristic fault related harmonics:
  - $f_{ednn1,2}$ – for dynamic eccentricity,
  - $f_{esnn1,2}$ – for static eccentricity,
  - $f_{nn}, f_{ednn1,2}, f_{esnn1,2}$ – for voltage asymmetry.

  For time period: $t = 0.9$ s
  - Signal of DWT approximation: a3 – for dynamic eccentricity (for wavelet filter: 'db45').
  - Signal of DWT approximation: a1 – for static eccentricity and voltage asymmetry (for wavelet filter: 'db45').

  The following parameters of the time-frequency analysis were set:

  A. Gabor's transform

  Base function $g(t)$: Blackman's window.

  Parameters: $\Delta M = 4$ – time step; $\Delta N = 4$ – frequency step.

  B. STFT transform

  Analysis time window function $\gamma(t)$: Hanning's window.

  Window length M : $M = 512$ samples $\Rightarrow M \cong 0.1$ s, with $F_s = 5000$ samples per second

  C. Wigner–Ville transform

  Window length M : $M = 512$ samples $\Rightarrow M \cong 0.1$ s, with $F_s = 5000$ samples per second

  D. Continuous wavelet transform (CWT)

  Morlet's wavelet was selected.

In the case of time-frequency analyses performed with continuous wavelet transform (CWT) scale related to instantaneous frequency of characteristic fault harmonics for time t, obtained from the graph in Fig. 14.

For time-frequency analyses performed with CWT, a scale range from 1 to 64 with 0.125 step was set.

This scale range allows obtaining a better resolution of CWT transform for the middle frequencies range containing the examined harmonics as shown in figure below.

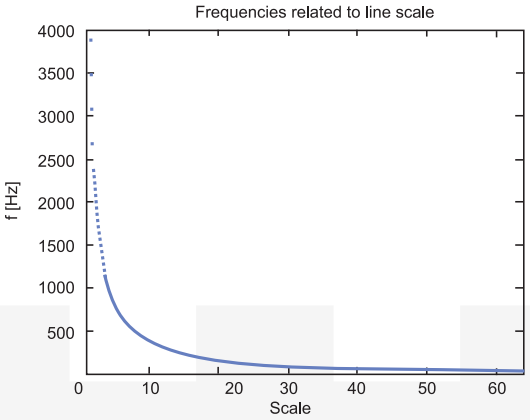

Fig. 14. Frequency vs. Scale curve for Morlet wavelet for S = 1:0,125:64

Programs for performing Gabor's, STFT and Wigner–Ville's transforms were based on algorithms given in [1]. For performing DWT and CWT and transforms and designing the notch filter, library functions of MATLAB were used.

– *Multi-resolution analysis with DWT*

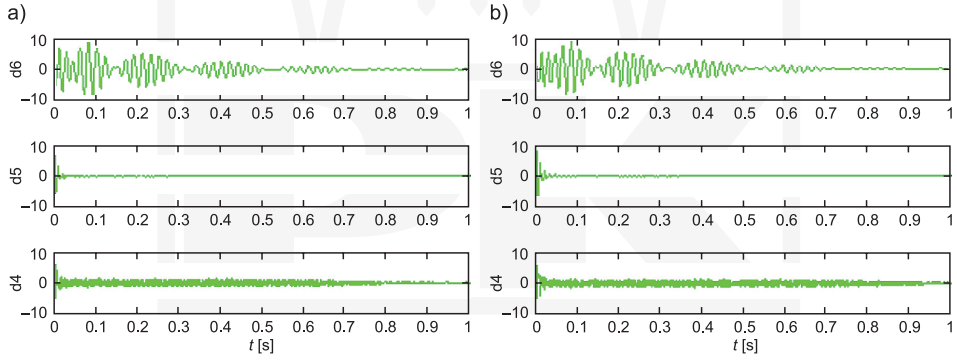

Fig. 15. Dynamic eccentricity detection: analysis of d4 and d5: a) i_sym, b) i_de

Table 3

Quantitative factors for ED detection: analysis of d4 and d5

Case	E (db45)	
	Decomposition signal	
	d5	d4
i_sym	5.4724	0.3529
i_de	7.1124	0.3639

Case	W [%] (db45)	
	Decomposition signal	
	d5	d4
i_de	29.97	3.12

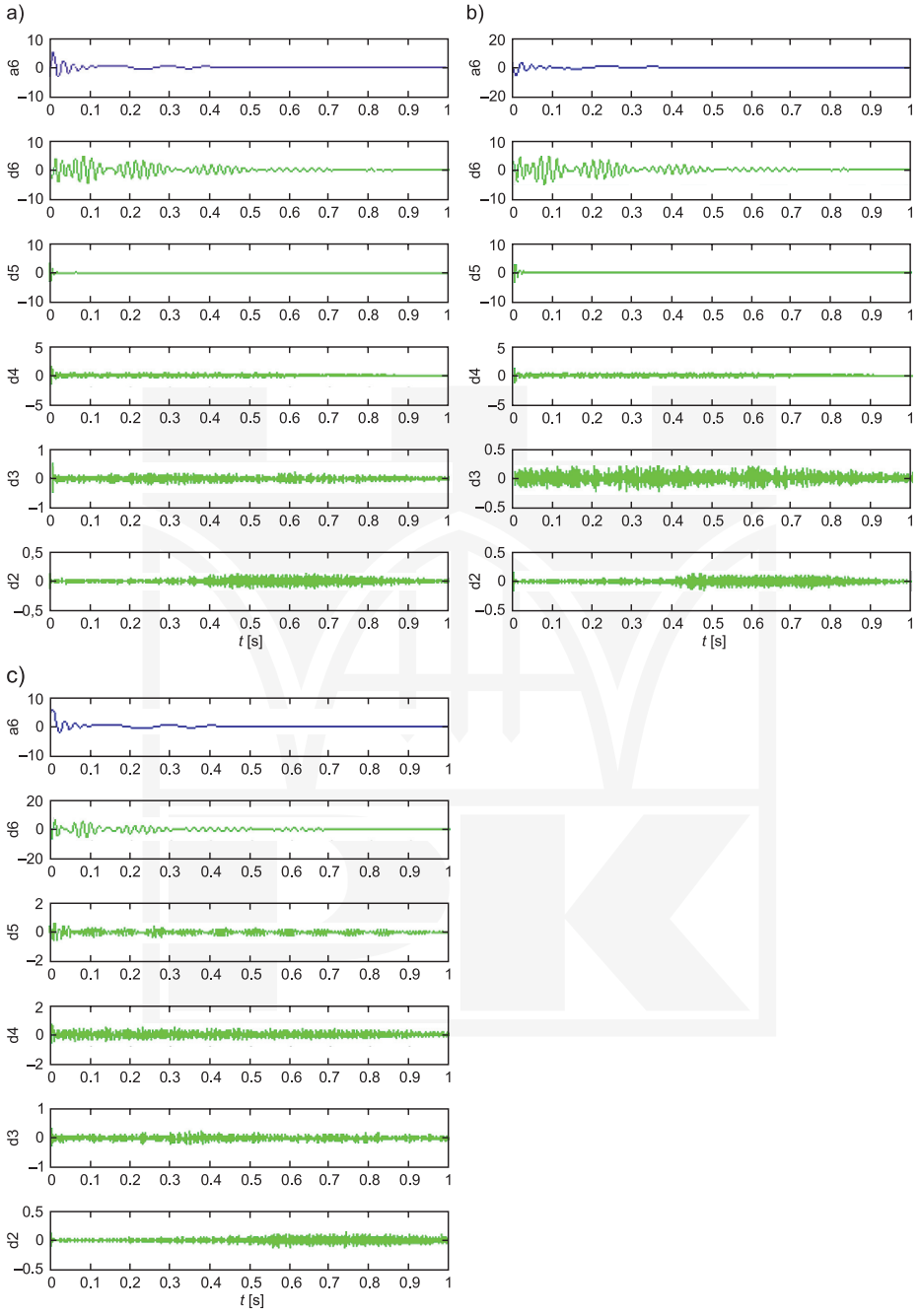

Fig. 16. Detection of static eccentricity and voltage asymmetry: analysis d2 – a6: a) i_sym, b) i_se, c) i_senn

Table 4

Quantitative factors for ES and NN detection: analysis d2 – a6

Case	*E* (db45)				
	Decomposition signal				
	a6	d5	d4	d3	d2
i_sym	83.8955	5.4724	0.3529	0.019	0.004
i_se	85.2914	5.118	0.2886	0.015	0.0037
i_senn	70.1393	0.2611	0.1306	0.0127	0.0029

Case	*W* [%] (db45)				
	Decomposition signal				
	a6	d5	d4	d3	d2
i_se	1.66	6.48	18.22	21.05	7.50
i_senn	16.40	95.23	62.99	33.16	27.50

– *Time-frequency analysis on TF planes*

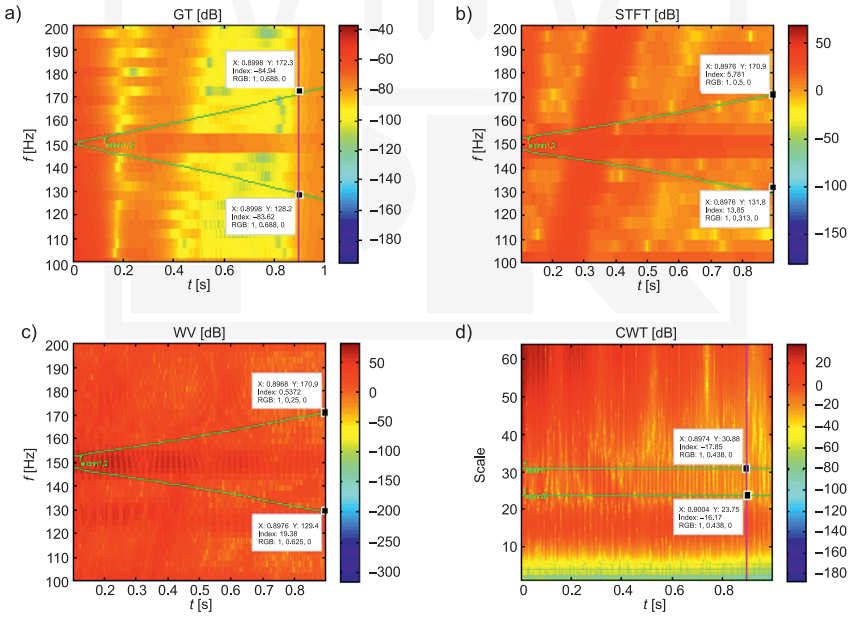

Fig. 17. Signal of DWT approximation: a3 – for ED: i_de:
a) GT; b) STFT; c) WV; d) CWT

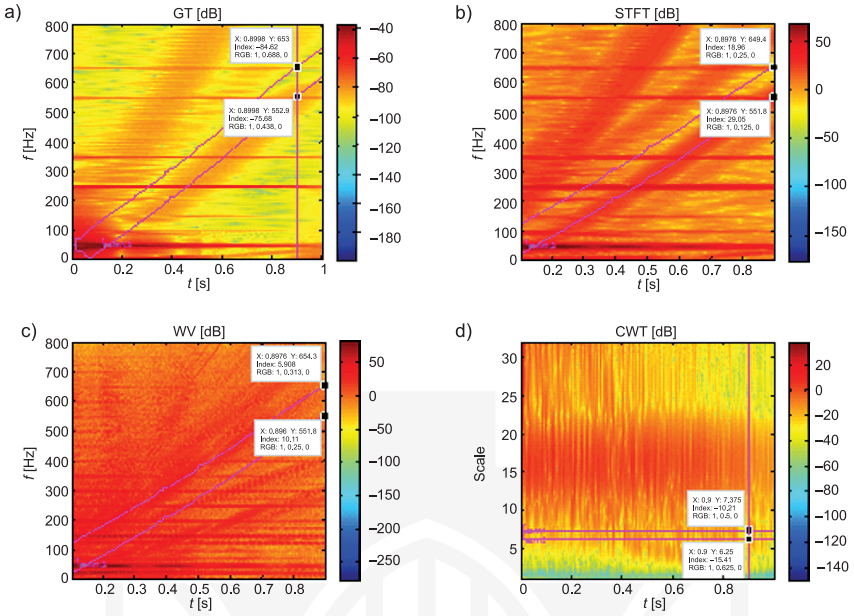

Fig. 18. Signal of DWT approximation: a1 – for ES: i_se:
a) GT; b) STFT; c) WV; d) CWT

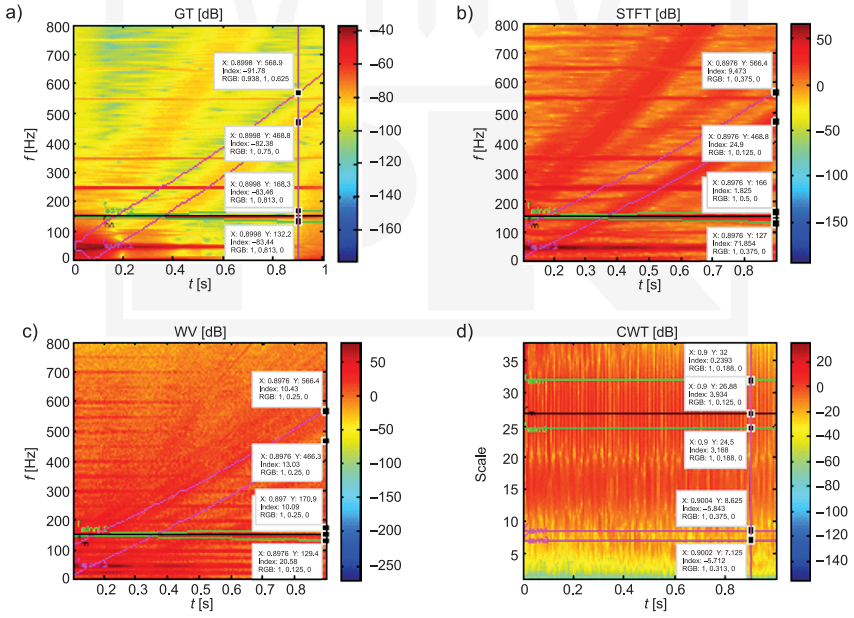

Fig. 19. Signal of DWT approximation: a1 – for ES and NN: i_senn:
a) GT; b) STFT; c) WV; d) CWT

Table 5

Quantitative factors for particular signals of DWT approximations for dynamic eccentricity occurrence case

Case	*GT* (a3: db45): *E* [dB]	
	Harmonic	
	fednn1	fednn2
i_sym	–92.1	–97.21
i_de	–83.62	–84.94
	STFT (a3: db45): *E* [dB]	
i_sym	–2.531	–14.95
i_de	13.85	5.781
	WV (a3: db45): *E* [dB]	
i_sym	8.798	–26.61
i_de	19.38	0.5372
	CWT (a3: db45): *E* [dB]	
i_sym	–19.91	–21.28
i_de	–17.85	–16.17

Case	*GT* (a3: db45): Δ*E* [dB]	
	Harmonic	
	fednn1	fednn2
i_de	8.48	12.27
	STFT (a3: db45): Δ*E* [dB]	
i_de	16.381	20.731
	WV (a3: db45): Δ*E* [dB]	
i_de	10.582	27.1472
	CWT (a3: db45): Δ*E* [dB]	
i_de	2.06	5.11

Table 6

Quantitative factors for particular signals of DWT approximations for static eccentricity and voltage asymmetry considered as distortion occurrence case

Case	*GT* (a1: db45): *E* [dB]				
	Harmonic				
	fednn1	fednn2	fesnn1	fesnn2	fnn
i_sym	–92.67	–98.37	–87.53	–103.8	–85.06
i_se			–75.68	–84.62	
i_senn	–83.44	–83.46	–82.38	–91.78	–61.8
	STFT (a1: db45): *E* [dB]				
i_sym	–2.532	–14.97	21.62	–5.074	19.58
i_se			29.05	18.96	
i_senn	7.854	1.825	24.9	9.473	41.37
	WV (a1: db45): *E* [dB]				
i_sym	8.809	-8.79	–5.753	–5.628	13.83
i_se			10.11	5.908	
i_senn	20.58	10.09	13.03	10.43	35.27

	CWT (a1: db45): E [dB]				
i_sym	–19.58	–21.73	–19.36	–24.57	–17.58
i_se			–10.21	–15.41	
i_senn	0.2393	3.168	–5.843	–5.712	3.934

Case	***GT* (a1: db45): Δ*E* [dB]**				
	Harmonic				
	fednn1	fednn2	fesnn1	fesnn2	fnn
i_se			11.85	19.18	
i_senn	9.23	14.91	5.15	12.02	23.26
	STFT (a1: db45): Δ*E* [dB]				
i_se			7.43	24.034	
i_senn	10.386	16.795	3.28	14.547	21.79
	WV (a1: db45): Δ*E* [dB]				
i_se			15.863	11.536	
i_senn	11.771	18.88	18.783	16.058	21.44
	CWT (a1: db45): Δ*E* [dB]				
i_se			9.15	9.16	
i_senn	19.8193	24.898	13.517	18.858	21.514

6. Conclusion

The aim of performed analyses was the efficiency evaluation of the presented methodology of detecting dynamic and static eccentricity. Supply voltage asymmetry was considered as distortion of harmonics based method of static eccentricity detection. The obtained results of the performed analyses are as follows:

– Multi-resolution analysis with DWT:

  In the obtained DWT decompositions, one can notice changes showing the occurrence of particular faults. For slip dependent harmonics, these changes are details covering the highest ranges at the end of start-up– d4 for dynamic eccentricity, d2 and d3 for static eccentricity and d2-d5 for static eccentricity with voltage asymmetry.

  In the case of percentage energy of DWT signals, dynamic eccentricity occurrence causes the rise of the percentage energy of signals d4 and d5, however, when static eccentricity occurs, the percentage energy of details d2-d5 decreases. In the case of the simultaneous occurrence of static eccentricity and voltage asymmetry, the decrease of the percentage energy of details d2-d5 becomes significant.

In the case of TF analyses, when analyzing energies of the examined harmonics one can notice their increase when a fault occurs. It happens for all transforms both for a3 approximation for dynamic eccentricity and for a1 approximation for static eccentricity with voltage asymmetry.

In the obtained transforms, harmonics $f_{ednn1,2}$ are not clearly visible. The waveform of $f_{esnn1,2}$ harmonic is visible in all TF transforms except that in Wigner–Ville's transform, one can distinguish waveforms of two harmonics. Harmonic f_{nn} waveform is also clearly visible.

It can be concluded that the proposed methodology is effective in the detection of the examined faults both for multi-resolution analysis with DWT and time-frequency analyses on the TF plane.

General observations and conclusions can be formed:

- With TF analyses using Gabor transform, Wigner–Ville's transform, STFT and CWT, all examined machine faults were successfully diagnosed, thanks to the localization of typical slip dependent harmonics, which is a TMCSA method. In the current signal's decompositions obtained by DWT multi-resolution analysis, it is more difficult to observe characteristic features of faults. Also, analysis of wavelet signals percentage energy values, one cannot find any particular dependencies related to fault occurrence.
- Using the notch filter in order to remove the base harmonic of current signal of frequency equal to that of supply voltage, made it easier to distinguish characteristic fault harmonics in the time-frequency transforms. Although using the notch filter allowed the removal of a significant part of the base harmonic, the filtration is not ideal and a part of the base harmonic remained. This combined with the Gibbs effect, which is connected with filtration and signal processing, still causes the deterioration of the obtained transforms and decompositions' quality.
- In conclusion, one can say that using the presented methodology of time-frequency analysis application in fault detection of cage induction machines and simple data acquisition system for collecting phase current and rotational speed signal, it was possible to detect the examined machine's faults. Also, using a rotational speed signal allowed obtaining the actual harmonics' waveforms and localize them of TF plane in specified moment, especially in cases where those harmonics were hard to observe which happened for dynamic eccentricity.

References

[1] Zieliński T.P., *Cyfrowe przetwarzanie sygnałów. Od teorii do zastosowań*, WKŁ, Warszawa 2005.

[2] Augustyniak P., *Transformacje falkowe w zastosowaniach elektrodiagnostycznych*, Wydawnictwo AGH, Kraków 2003.

[3] Białasiewicz J.T., *Falki i aproksymacje*, WNT, Warszawa 2000.

[4] Zygarlicka M., *Wybrane metody przetwarzania obrazów w analizach czasowo-częstotliwościowych na przykładzie zakłóceń w sieciach elektroenergetycznych*, rozprawa doktorska, Politechnika Opolska, Opole 2011.

[5] Szabatin J., *Podstawy teorii sygnałów*, WKŁ, Wydawnictwo V, Warszawa 2007.
[6] Riera-Guasp M., Pineda-Sánchez M., Perez-Cruz J., Puche-Panadero R., Roger-Folch J., Antonino-Daviu J., *Diagnosis of Induction Motor Faults via Gabor Analysis of the Current in Transient Regime*, IEEE Transactions on Instrumentation and Measurement, Dec. 2012, Vol. 61, No. 6, 1583-1596.
[7] Pineda-Sánchez M., Riera-Guasp M., Pons-Llinares J., Climente-Alarcón V., Perez-Cruz J., *Diagnosis of Induction Machines under Transient Conditions through the Instantaneous Frequency of the Fault Components*, XIX International Conference on Electrical Machines – ICEM, Rome 2010.
[8] Riera-Guasp M., Antonino-Daviu J.A., Pineda-Sanchez M., Puche-Panadero R., Perez-Cruz J., *A General Approach for the Transient Detection of Slip-Dependent Fault Components Based on the Discrete Wavelet Transform*, IEEE Transactions on Industrial Electronics, Dec. 2008, Vol. 55, No. 12, 4167-4180.
[9] Riera-Guasp M., Antonino-Daviu J.A., Roger-Folch J., Pilar Molina Palomares M., *The Use of the Wavelet Approximation Signal as a Tool for the Diagnosis of Rotor Bar Failures*, IEEE Transactions on Industry Applications, May/June 2008, Vol. 44, No. 3, 716-726.
[10] Antonino-Daviu J.A., Riera-Guasp M., Pineda-Sanchez M., Pérez R. B., *A Critical Comparison Between DWT and Hilbert–HuangBased Methods for the Diagnosis of Rotor Bar Failures in Induction Machines*, IEEE Transactions on Industry Applications, Sep./Oct. 2009, Vol. 45, No. 5, 1794-1803.
[11] Pineda-Sanchez M., Riera-Guasp M., Antonino-Daviu J.A., Roger-Folch J., Perez-Cruz J., Puche-Panadero R., *Diagnosis of Induction Motor Faults in the Fractional Fourier Domain*, IEEE Transactions on Instrumentation and Measurement, Aug. 2010, Vol. 59, No. 8, 2065-2075.
[12] Wolkiewicz M., Kowalski Cz.T., *Nieinwazyjne metody wczesnego wykrywania zwarć zwojowych w silniku indukcyjnym zasilanym z przemiennika częstotliwości, cz. I*, BOBRME Komel, Zeszyty Problemowe – Maszyny Elektryczne, 2010, nr 87, 145-150.
[13] Kowalski Cz.T., Kanior W., *Ocena skuteczności analiz FFT, STFT i falkowej w wykrywaniu uszkodzeń wirnika silnika indukcyjnego*, Prace Naukowe Instytutu Maszyn, Napędów i Pomiarów Elektrycznych Politechniki Wrocławskiej Nr 60, Studia i Materiały Nr 27, 2007.
[14] Help programu MATLAB R2011b.